Exploration of Bis(Arylimidazole) Iridium Picolinate Complexes

Dr. Aron J. Huckaba,[a] Sadig Aghazada,[a] Dr. Iwan Zimmermann,[a] Dr. Giulia Grancini,[a] Dr. Natalia Gasilova,[a] Dr. Pascal Schouwink,[a] Prof. Dr. Mohammad K. Nazeeruddin [a,*]

a: Ecole Polytechnique Federale de Lausanne Valais Wallis, Rue de l'Indutrie 17, 1950 Sion, Valais, Switzerland. E-mail: mdkhaja.nazeeruddin@epfl.ch

KEYWORDS. Emissive Materials, Ir Complexes, Phosphorescent Materials, Physical Organic Chemistry, Imidazole Complexes

Supporting Information Placeholder

ABSTRACT: The straightforward synthesis and photophysical properties of a new series of heteroleptic Iridium (III) bis(2-arylimidazole) picolinate complexes is reported. Each complex has been characterized by NMR, UV-Vis, cyclic voltammetry, and the emissive properties of each is described. By systematically modifying first the cyclometallating aryl group on the arylimidazole ligand and then the picolinate ligand, the ramifications of ligand modification in these complexes was better understood through the construction of a structure-property relationship.

In the search for efficient light-emitting devices, Organic light emitting diodes (OLED) offer a full-spectrum inexpensive option, due to development of heavy atom emitters. Spin-orbit coupling (SOC) is strong in third row elements and allows for theoretical device efficiency near unity by utilizing singlet and triplets for light generation.[1,2] Ir complexes have been successful thus far, thanks to room temperature emissiion, strong SOC that allows for efficient phosphorescence from its ^{3}MLCT state, μs time range excited state lifetime, and high photoluminescence quantum yield (PLQY).[3,4,5,6]

Ir (III) emitters exhibiting emission of every color, especially green and red, have been synthesized to date; most have green to red colored emission bands. In the blue or violet emission, however, has been much more rare.[5] Current state of the art blue emitters have structures such as $(dfppy)_2Ir(pic)$, FirPic),[7,8] where dfppy = 2,4-difluorophenylpyridine and pic = picolinate, $(1\text{-Aryl-NHC})_3$,[9] where NHC = N-heterocyclic carbene, or $(2\text{-Arylimidazole})_3$ (Figure 1).[10,11] Each class of emitter has its drawbacks, however, such as low color-purity, poor stability, or poor tunability. In FirPic, the strongly withdrawn difluorophenyl- moiety stabilizes the molecular ground state (which lies on the phenyl ring) more than the excited state (which lies on the pyridine ring).[12,13] Such energy level tuning widens the HOMO-LUMO gap, thus increasing emission energy to the blue region. Slective functionalization of either cyclometallating phenyl or picolinate ligand has been shown to modify emission energy, PLQY, excited state lifetime, etc.

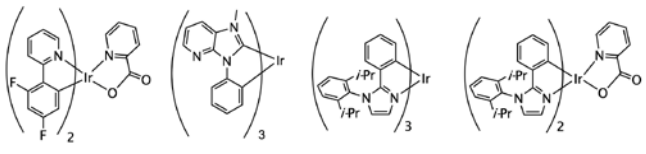

Figure 1. Structures of State of the Art Iridium Complexes and Iridium Complexes Investigated in this Study.

In $(1\text{-Aryl-NHC})_3$, sufficiently withdrawing NHC moieties can harbor a high energy excited state, leading to blue emission. In $(2\text{-Arylimidazole})_3$ complexes, a very high energy excited state lies on the wingtip aryl moiety, leading to blue emission.[14] Both of these types of complexes are synthetically more challenging to modify than arylpyridine complexes. Accordingly, many fewer studies have investigated the chemistry of these high-performing ligands,[15,16] especially in heteroleptic complexes.[17,18] Therefore, expanding the chemistry and photophysical understanding towards developing a deeper understanding of Iridium emitter structure-property relationshipsis a worthy goal for investigation. We report the synthesis and characterization of a series of functionalized heteroleptic bis(2-arylimidazole) Iridium (III) picolinate complexes that indicate beneficial and detrimental substitution patterns in these complexes.

Experimental Section

General Information: All commercially obtained reagents were used as received. Unless otherwise noted, all reactions were performed under a N_2 atmosphere. Thin-layer chromatography (TLC) was conducted with Sigma T-6145 pre-coated TLC Silica gel 60 F_{254} aluminum sheets and/or visualized with UV and potassium permanganate staining. Flash column chromatography was performed as described by Still using Silicycle P60, 40-63 μm (230-400 mesh).[19] ^{1}H NMR spectra were recorded on a Bruker AVIII-HD (400 MHz or 200 MHz), and are reported in ppm using solvent as an internal standard ($CDCl_3$ at 7.26 ppm). Data reported as: s = singlet, d = doublet, t = triplet, q = quartet, p = pentet, m = multiplet, b = broad, ap = apparent; coupling constant(s) in Hz; integration. UV-Vis spectra were measured with an LS-55 spectrometer. Cyclic voltammetry was measured with a Biologic S-200 potentiostat. Mass spectra were recorded on a Bruker Microflex MALDI-TOF or ESI mass spectrometer. 2,4,6-triisopropylaniline prepared according to literature procedure.[20] Single crystal X-Ray diffraction measurements were made on a Bruker Venture SCXRD instrument.

General procedure for imidazole formation

*1-(2',6'-diisopropylphenyl)imidazole (**1**).*[21] A 1 L roundbottom flask equipped with a stirbar was charged with 750 mL MeOH, sparged vigorously with N_2. After 20 min, 2,6-diispropylaniline (20 mL, 18.8 g, 106 mmol) and glyoxal (14.4 mL, 106 mmol, 40% in H_2O) added and let stir at rt. After 16h, large yellow crystals were observed. To this suspension, NH_4Cl (5.79 g, 212 mmol) added, a reflux condenser attached, and the solution warmed to reflux with stirring. Once the crystals had dissolved, formaldehyde (16 mL, 212 mmol, 37.5% in H_2O) added, heating continued. After 1.5 h, 85% H_3PO_4 (25 mL) added, allowed to continue to stir at reflux, and monitored by TLC. After 6h, the flask cooled to rt, then 0°C and pH adjusted to 9 with 15% KOH. Extracted with Et_2O (3x 250 mL), washed with H_2O (3x 500 mL), concentrated on rotary evaporator after drying with $MgSO_4$. Submitted to column chromatography using 650 mL SiO_2, gradient Hexanes to 30% EtOAc:Hexanes. Product spot concentrated to yield an off-white solid (12.4 g, 51% yield). ^{1}H NMR (400 MHz, $CDCl_3$) δ 7.53 (s, 1H), 7.49 (d, J = 8 Hz, 1H), 7.30 (d, 7.1 Hz, 3H), 6.99 (s, 1H), 2.45 (m, J = 4.8 Hz, 2H), 1.19 (d, J = 4.8 Hz, 12H).

1-(2',4',6'-triisopropylphenyl)imidazole (**2**). Reaction performed as for compound **1**, yield: 5.0 g, 52%. ^{1}H NMR (400 MHz, $CDCl_3$) δ 7.52 (s, 1H), 7.49 (s, 1H), 7.27 (s, 2H), 6.77 (s, 1H), 2.85 (m, J = 4.8 Hz, 1H), 2.55 (m, J = 6.9 Hz, 2H), 1.28 (d, J = 6.9 Hz, 6H), 1.13 (d, J = 7.0 Hz, 6H), 1.10 (d, J = 4.8 Hz, 6H). ^{13}C NMR (100 MHz, $CDCl_3$) δ 150.5, 146.3, 138.8, 130.8, 129.4, 121.8, 35.5, 28.3, 24.6, 24.5, 24.2.

General procedure for Negishi coupling

*1-(2',6'-diisopropylphenyl)-2-phenylimidazole (**3**).*[21] A flame dried schlenk flask equipped with a stirbar was charged with compound **1** (1.0 g, 4.34 mmol) and dry THF (5 mL), and allows to cool to 0°C with stirring. After 15 min, butyllithium (1.74 mL, 2.5 M in hexanes) added via syringe, let stir at 0°C. After 30 min, $ZnCl_2$ (3.2 mL, 1.9M in 2Me-THF) added via syringe, let stir at 0°C. After 30 min, solution allowed to warm to rt, then warmed to 40°C. Concentrated total volume to 4 mL and added dry toluene (4 mL), then iodobenzene (0.84 g, 0.46 mL, 4.1 mmol) and $Pd(PPh_3)_4$ (0.20 g, 0.17 mmol, 4% catalyst loading). Solution warmed to 90°C with stirring and monitored by TLC. After 21h, the reaction was cooled to rt and H_2O (5mL) added. Washed with 10% HCl (25 mL), dried with $MgSO_4$. Concentrated on rotary evaporator. Submitted to column chromatography using 400 mL SiO_2, gradient hexanes to 20% EtOAC:Hexanes. Product fractions concentrated to yield a beige solid (1.1 g, 87%). ^{1}H NMR (400 MHz, C_6D_6) δ 7.82 (d, J = 7.1 Hz, 2H), 7.45 (d, J = 0.9 Hz, 1H), 7.18 (t, J = 7.8 Hz, 1H), 7.00 (d, J = 7.9 Hz, 2H), 6.95 (at, J = 6.9 Hz, 2H), 6.91 (ad, J = 7.0 Hz, 1H), 6.67 (d, J = 1.1 Hz, 1H), 2.58 (m, J = 6.9 Hz, 2H), 1.06 (s, 9H), 0.97 (d, J = 6.9 Hz, 6H), 0.83 (d, J = 6.9 Hz, 6H).

1-(2',4',6'-triisopropylphenyl)-2-phenylimidazole (**4**). Reaction performed as for compound **3**, yield: 1.3 g, 65%. ^{1}H NMR (400 MHz, $CDCl_3$) δ 7.42-7.39 (m, 2H), 7.29 (s, 1H), 7.18-7.16 (m, 3H), 7.07 (s, 2H), 6.93 (s, 1H), 2.96 (m, J = 6.9 Hz, 1H), 2.44 (m, J = 6.9 Hz, 2H), 1.30 (d, J = 7.0 Hz, 6H), 1.10 (d, J = 6. Hz, 6H), 0.88 (d, J = 7.0 Hz, 6H). ^{13}C NMR (100 MHz, $CDCl_3$) δ 150.7, 147.3, 145.7, 132.2, 130.7, 129.0, 128.4, 128.3, 127.4, 124.0, 122.4, 34.6, 31.9, 28.5, 25.4, 24.3, 23.1, 22.9.

*1-(2,6-diisopropylphenyl)-2-(4''-tertbutylphenyl)imidazole (**5**).* Reaction performed as for compound **3**, yield: 1.2 g, 81%. ^{1}H NMR (400 MHz, C_6D_6) δ 7.79 (d, J = 7.8 Hz, 2H), 7.45 (d, J = 1.1 Hz, 1H), 7.23 (t, J = 7.8 Hz, 1H), 7.08 (at, J = 8.7 Hz, 4H), 6.71 (d, J = 1.1 Hz, 1H), 2.58 (m, J = 6.8 Hz, 2H), 1.06 (s, 9H), 0.97 (d, J = 6.9 Hz, 6H), 0.83 (d, J = 6.9 Hz, 6H). ^{13}C NMR (100 MHz, C_6D_6) δ 150.6, 146.8, 146.0, 135.1, 129.6, 129.4, 128.5, 127.8, 127.7, 127.5, 127.4, 126.8, 124.9, 124.11, 123.0, 34.1, 30.8, 28.1, 24.6, 22.5.

General Procedure for chloro-bridged Iridium dimer formation

di-μ-chlorobis(*1-(2',6'-diisopropylphenyl)-2-phen-2''-ylimidazol-3-yl)diiridium (**6**).* A sealable pressure tube equipped with a stirbar was charged with compound **3** (0.63 g, 2.05 mmol), tridecane (5 mL), sparged with N_2. After 35 minutes, $[Ir(COD)Cl]_2$ (0.32 g, 0.47 mmol) added and the tube sealed under N_2. The tube was allowed warmed to 240°C with stirring and monitored by TLC. After 15h, much yellow ppt observed. Crude reaction submitted directly to column chromatography using 350 mL SiO_2 and a gradient of hexanes to 20% EtOAc:Hexanes. Product spot concentrated to yield a bright yellow solid (0.60 g, 77%). ^{1}H NMR (400 MHz, $CDCl_3$) δ 7.76 (s, 4H), 7.57 (t, J = 7.6 Hz, 4H), 7.45-7.38 (m, 8H), 6.51-6.32 (m, 8H), 6.92 (s, 4H), 6.52 (t, J = 7.2 Hz, 4H), 6.34 (m, 8H), 6.06 (d, J = 7.5 Hz, 4H), 3.0-2.83 (m, 8H), 1.37-1.21 (m, 42H), 0.94 (d, J = 6.8 Hz, 16H). ^{13}C NMR (100 MHz, $CDCl_3$) δ 158.9, 146.8, 146.7, 135.0, 135.1, 133.7, 131.9, 130.6, 127.9, 124.8, 124.6, 121.7, 120.2, 29.0, 28.7, 25.2, 24.6, 24.0, 23.4.

di-μ-chlorobis(*1-(2',4',6'-triisopropylphenyl)-2-phen-2''-ylimidazol-3-yl)diiridium (**7**).* Reaction performed as for compound **7**, yield: 0.265 g, 52%. ^{1}H NMR (400 MHz, C_6D_6) δ 8.17 (d, J = 1.5 Hz, 4H), 7.22 (t, J = 7.7 Hz, 4H), 7.13 (dd, J = 7.4 Hz, 1.5 Hz, 4H), 7.06 (dd, J = 7.7 Hz, 1.4 Hz, 4H), 6.89 (d, J = 1.5 Hz, 4H), 6.86 (dd, J = 7.8 Hz, 1.1 Hz, 4H), 6.69 (dt, J = 6.6 Hz, 1.5 Hz, 4H), 6.51 (dt, J = 7.3 Hz, 1.2 Hz, 4H), 6.42 (dd, J = 7.7 Hz, 1.5 Hz, 4H), 3.01 (m, J = 6.9 Hz, 8H), 1.13 (at, J = Hz, 24H), 1.02 (d, J = 6.9 Hz, 12H), 0.77 (d, J = 6.9 Hz, 12H). ^{13}C NMR (100 MHz, $CDCl_3$) δ 158.9, 151.1, 146.7, 146.4, 146.2, 145.1, 135.3, 131.9, 131.5, 129.0, 128.9, 127.8, 127.7, 122.6, 122.5, 122.4, 121.7, 120.6, 120.4, 119.7, 35.0, 34.7, 31.9, 29.1, 28.8, 27.2, 25.6, 25.2, 25.1, 24.7, 24.4, 24.3, 24.1, 23.5, 22.9. HRMS (CI-MS): Theo. for $C_{96}H_{117}Cl_2Ir_2N_8$, $[M+H]^+$: 1801.8353, found for $C_{54}H_{63}IrN_5O_2$, $[M+H]^+$: 1801.8354.

di-μ-chlorobis(*1-(2',6'-diisopropylphenyl)-2-(4''-tertbutylphen-2''-yl)imidazol-3-yl)diiridium (**8**).* Reaction performed as for compound **7**, yield: 0.235 g, 80%. ^{1}H NMR (200 MHz, $CDCl_3$) δ 7.83 (m, 2H), 7.63-7.26 (m, 18H), 6.89 (bs, 4H), 6.51-6.32 (m, 8H), 5.91 (bs, 4H), 2.85 (bs, 4H), 1.54 (s, 24H), 1.30 (s, 24H), 1.04 (s, 45H). ^{13}C NMR (100 MHz, $CDCl_3$) δ 159.3, 150.0, 149.9, 147.4, 147.3, 146.9, 146.3, 133.8, 131.9, 130.5, 129.1, 128.7, 128.4, 127.4, 124.6, 124.6, 121.1,

119.9, 117.0, 34.5, 34.5, 31.7, 31.6, 31.6, 28.9, 28.8, 23.9, 23.8, 23.8, 25.1.

General Procedure for Heteroleptic Ir (III) Picolinate Synthesis

bis(*1-(2',6'-diisopropylphenyl)-2-phen-2''-ylimidazol-3-yl)iridium (III) picolinate (***9***).* 25 mL roundbottom flask equipped with a stirbar and reflux condenser was charged with dichloromethane (15 mL), compound **6** (0.25 g, 0.015 mmol) and sparged with N_2. After 10 minutes, 2-picolinic acid (0.006 g, 0.045 mmol) and NEt_3 (0.006 g, 0.011 mL, 0.075 mmol) added and the reaction warmed to reflux with stirring and monitored by TLC. After 18h, the yellow solution was concentrated and passed through an SiO_2 plug using first 20% EtOAc:Hexanes, then acetone. Product fractions concentrated to yield a bright yellow solid (0.060 g, 65%, based on picolinic acid). ^{1}H NMR (400 MHz, $CDCl_3$) δ 8.34 (d, J =7.5 Hz, 1H), 7.91-7.83 (m, 2H), 7.53 (td, J =2.5 Hz, 7.2 Hz, 4H), 7.38-7.24 (m, 8H), 6.88 (d, J = 1.6 Hz, 1H), 6.81 (d, J = 1.7 Hz, 1H), 6.64-6.58(m, 5H), 6.47-6.38 (m, 2H), 6.34 (d, J = 1.7 Hz, 1H), 6.1 (d, J = 7.8 Hz, 1H), 6.05 (d, J = 7.8 Hz, 1H), 2.81-2.56 (m, 4H), 1.35-0.9 (m, 24H). ^{13}C NMR (100 MHz, $CDCl_3$) δ 173.9, 159.6, 158.2, 153.4, 149.1, 148.1, 147.1, 146.6, 146.4, 146.3, 145.3, 137.0, 135.5, 135.4, 133.7, 133.2, 133.1, 133.0, 130.8, 130.7, 128.3, 128.2, 127.7, 127.1, 126.0, 125.3, 124.9, 124.8, 124.8, 124.7, 124.6, 122.8, 122.3, 121.8, 121.6, 120.5, 120.1, 28.8, 28.7, 28.5, 25.2, 24.5, 24.0, 23.8, 23.6, 23.5.

bis(*1-(2',6'-triisopropylphenyl)-2-(4''-tertbutylphen-2''-yl)imidazol-3-yl)iridium (III) picolinate (***10***).* Reaction performed as for compound **9** with the exception of 2 equiv picolinate and NEt_3 used, yield: 0.020 g, 15%. ^{1}H NMR (400 MHz, $CDCl_3$) δ 8.29 (d, J = 7.9 Hz, 1H), 7.82 (t, J = 7.7 Hz, 1H), 7.64 (d, J = 5.2 Hz, 1H), 7.52 (t, J = 7.7 Hz, 2H), 7.38-7.26 (m, 6H), 7.21 (t, J = 6.4 Hz, 1H), 6.83 (s, 1H), 6.81 (s, 1H), 6.77 (s, 1H), 6.54 (d, J = 8.2 Hz, 1H), 6.47 (d, J = 8.2 Hz, 1H), 6.39 (s, 1H), 6.03 (d, J = 8.2 Hz, 1H), 5.99 (d, J = 8.2 Hz, 1H), 2.85 (m, 1H), 2.73 (m, 1H), 2.49 (m, 1H), 1.85 (m, 1H), 2.05 (m, 4H), 1.26-0.8 (m, 68H). ^{13}C NMR (100 MHz, $CDCl_3$) δ 173.9, 159.8, 158.4, 153.7, 151.1, 150.3, 148.4, 147.6, 147.5, 146.7, 146.6, 146.5, 145.0, 136.6, 133.1, 133.1, 132.7, 132.6, 131.0, 130.7, 127.7, 126.8, 125.9, 125.1, 124.9, 124.7, 124.4, 122.3, 121.8, 121.3, 121.2, 117.9, 117.3, 34.5, 31.7, 31.7, 31.6, 30.0, 28.9, 28.8, 28.6, 28.4, 25.3, 25.2, 25.1, 24.5, 23.8, 23.7, 23.7. HRMS (CI-MS): Theo. for $C_{56}H_{67}IrN_5O_2$, $[M+H]^+$: 1034.4919, found for $C_{56}H_{67}IrN_5O_2$, $[M+H]^+$: 1034.4930.

bis(*1-(2',4',6'-triisopropylphenyl)-2-phen-2''-ylimidazol-3-yl)iridium (III) picolinate (***11***).* Reaction performed as for compound **9** with the exception of 11 equiv picolinate and 17 equiv Net_3, yield: 0.050 g, 92%. ^{1}H NMR (400 MHz, $CDCl_3$) δ 8.26 (d, J = 7.7 Hz, 1H), 7.83-7.76 (m, 2H), 7.20-7.05 (m, 6H), 6.79 (s, 1H), 6.72 (s, 1H), 6.81 (d, J = 1.5 Hz, 1H), 6.54-6.30 (m, 7H), 6.25 (s, 1H), 6.06-5.94 (m, 2H), 2.94 (m, 3H), 2.05 (m, 4H), 1.25-0.7 (m, 36H). ^{13}C NMR (100 MHz, $CDCl_3$) δ 173.9, 159.6, 158.3, 153.5, 151.4, 151.2, 149.0, 148.1, 146.6, 146.1, 146.0, 145.9, 145.4, 136.9, 135.7, 135.5, 133.7, 133.2, 130.7, 128.1, 127.7, 127.0, 125.8, 125.2, 122.8, 122.7, 122.6, 122.5, 122.4, 122.3, 121.9, 121.8, 120.4, 120.0, 34.6, 29.9, 28.8, 28.8, 28.6, 25.2, 24.7, 24.7, 24.5, 24.3, 24.1, 23.9, 23.7, 23.6. HRMS (CI-MS): Theo. for $C_{54}H_{63}IrN_5O_2$, $[M+H]^+$: 1006.4606, found for $C_{54}H_{63}IrN_5O_2$, $[M+H]^+$: 1006.4619.

bis(*1-(2',6'-triisopropylphenyl)-2-(phen-2''-yl)imidazol-3-yl)iridium (III) 4-methylpicolinate (***12***).* Reaction performed as for compound **9** with the exception of 10 equiv picolinate and NEt_3 used, yield: 0.048 g, 43%. ^{1}H NMR (400 MHz, $CDCl_3$) δ 8.19 (s, 1H), 7.75 (d, J = 5.5 Hz, 1H), 7.54 (m, 2H), 7.36 (m, 5H), 7.08 (dd, J = 5.5 Hz, 2.0 Hz, 1H), 6.90 (d, J = 1.5 Hz, 1H), 6.82 (d, J = 1.5 Hz, 1H), 6.58 (m, 4H), 6.47 (t, J = 6.8 Hz, 1H), 6.42 (d, J = 6.8 Hz, 1H), 6.37 (d, J = 1.6 Hz 1H), 6.12 (d, J = 8.2 Hz, 1H), 6.06 (d, J = 8.2 Hz, 1H), 2.79 (m, 1H), 2.73 (m, 1H), 2.65 (m, 1H) 2.46 (s, 3H), 2.20 (m, 1H), 1.24 (d, J = 6.9 Hz, 3H), 1.22 (d, J = 6.9 Hz, 3H), 1.17 (d, J = 7.0 Hz, 3H), 1.11 (d, J = 6.9 Hz, 3H), 1.03 (d, J = 7.1 Hz, 3H), 0.95 (m, 9H). ^{13}C NMR (100 MHz, $CDCl_3$) δ 174.1, 159.6, 158.3, 152.8, 148.9, 148.6, 148.4, 147.1, 146.6, 146.5, 146.3, 145.6, 135.5, 135.4, 133.7, 133.2, 133.1, 133.1, 130.8, 130.7, 128.6, 128.2, 128.1, 127.8, 126.0, 125.3, 124.8, 124.8, 124.6, 124.5, 122.7, 122.2, 121.6, 121.6, 121.5, 120.3, 120.0, 28.8, 28.8, 28.7, 28.5, 25.2, 24.7, 24.6, 24.5, 24.0, 23.8, 23.6, 21.5. HRMS (CI-MS): Theo. for $C_{49}H_{53}IrN_5O_2$, $[M+H]^+$: 936.3823, found for $C_{49}H_{53}IrN_5O_2$, $[M+H]^+$: 936.3842.

bis(*1-(2',6'-triisopropylphenyl)-2-(phen-2''-yl)imidazol-3-yl)iridium (III) 4-trifluoromethylpicolinate (***13***).* Reaction performed as for compound **9** with the exception of 10 equiv picolinate and NEt_3 used, yield: 0.047 g, 40%. ^{1}H NMR (400 MHz, $CDCl_3$) δ 8.60 (s, 1H), 8.10 (d, J = 5.5 Hz, 1H), 7.55 (m, 2H), 7.42 (dd, J = 5.1, 2.1 Hz, 1H), 7.38-7.30 (m, 5H), 6.92 (d, J = 1.5 Hz, 1H), 6.84 (d, J = 1.5 Hz, 1H), 6.62 (m, 2H), 6.54-6.41 (m, 4H), 6.32 (d, J = 1.7 Hz, 1H), 6.11 (d, J = 8.0 Hz, 1H), 6.07 (d, J = 8.2 Hz, 1H), 2.79 (m, 1H), 2.80-2.56 (m, 3H) 2.15 (m, 1H), 1.21 (at, J = 6.9 Hz, 6H), 1.15 (d, J = 6.9 Hz, 3H), 1.10 (d, J = 7.0 Hz, 3H), 1.05 (d, J = 6.9 Hz, 3H), 1.03 (d, J = 7.1 Hz, 3H), 0.93 (m, 9H). ^{13}C NMR (100 MHz, $CDCl_3$) δ 172.4, 159.4, 158.2, 155.4, 150.1, 147.1, 147.0, 146.6, 146.4, 144.0, 138.4 (q, J = 34.9 Hz), 135.4, 135.2, 133.4, 133.2, 133.0, 132.9, 131.0, 130.8, 128.5, 128.3, 125.9, 125.2, 125.0, 124.9, 124.8, 124.6, 124.1, 122.9, 122.4, 122.1, 121.9, 121.3, 120.9, 120.6, 28.8, 28.8, 28.8, 28.8, 28.6, 28.6, 25.2, 24.7, 24.4, 24.0, 23.8, 23.7, 23.5. HRMS (CI-MS): Theo. for $C_{49}H_{50}IrN_5O_2F_3$, $[M+H]^+$: 990.3540, found for $C_{49}H_{50}IrN_5O_2F_3$, $[M+H]^+$: 990.3562.

bis(*1-(2',6'-triisopropylphenyl)-2-(phen-2''-yl)imidazol-3-yl)iridium (III) 4-methoxypicolinate (***14***).* Reaction performed as for compound **9** with the exception of 10 equiv picolinate and NEt_3 used, yield: 0.066 g, 58%. ^{1}H NMR (400 MHz, $CDCl_3$) δ 7.91 (d, J = 2.9 Hz, 1H), 7.64 (d, J = 6.1 Hz, 1H), 7.52 (m, 2H), 7.38-7.29 (m, 5H), 6.89 (d, J = 1.6 Hz, 1H), 6.81 (d, J = 1.5 Hz, 1H), 6.76 (dd, J = 6.1, 1.7 Hz, 1H), 6.61-6.51 (m, 4H), 6.46-6.37 (m, 3H), 6.09 (d, J = 8.0 Hz, 1H), 6.03 (d, J = 8.2 Hz, 1H), 3.93, (s, 3H), 2.75-2.55 (m, 3H), 2.2 (m, 1H), 1.21 (at, J = 6.9 Hz, 6H), 1.15 (d, J = 6.9 Hz, 3H), 1.09 (d, J = 7.0 Hz, 3H), 1.03 (d, J = 6.8 Hz, 3H), 1.03 (d, J = 7.1 Hz, 3H), 0.93 (m, 9H). ^{13}C NMR (100 MHz, $CDCl_3$) δ 173.8, 166.6, 159.7, 155.3, 149.5, 148.3, 147.1, 146.7, 146.5, 146.4, 145.6, 135.5 133.7, 133.2, 133.1, 133.2, 130.8, 130.7, 128.2, 128.1, 126.0, 125.4, 124.9, 124.5, 122.7, 122.3, 121.6, 120.3, 119.9, 114.7, 112.0, 56.18, 28.8, 28.7, 28.5, 25.2, 24.7, 24.5, 24.0, 23.9, 23.7, 23.5. HRMS (CI-MS): Theo. for $C_{49}H_{53}IrN_5O_3$, $[M+H]^+$: 952.3772, found for $C_{49}H_{53}IrN_5O_3$, $[M+H]^+$: 952.3796.

Results and Discussion

Synthesis of Iridium Complexes

To experimentally establish a structure-function relationship for this class of ligand, we envisioned a series of complexes with functionalization on both wingtip and cyclometallating phenyl moieties (Scheme 1). Wingtip-modified ligands were reached by first synthesizing the appropriate imidazole with reproducible yields near 50%, and then coupling the appropriate aryl bromide through a key Negishi coupling reaction. This smoothly and reproducible yielded each of the imidazole ligands **3**-**5** with good yields of 65-81%. After forming chloride-bridged iridium dimers with each ligand at high temperature in acceptable yields of 52-80%, heteroleptic picolinate complexes were obtained after ligation with commercially available picolinate ligands to form complexes **9**-**12** with yields between 15-92%.

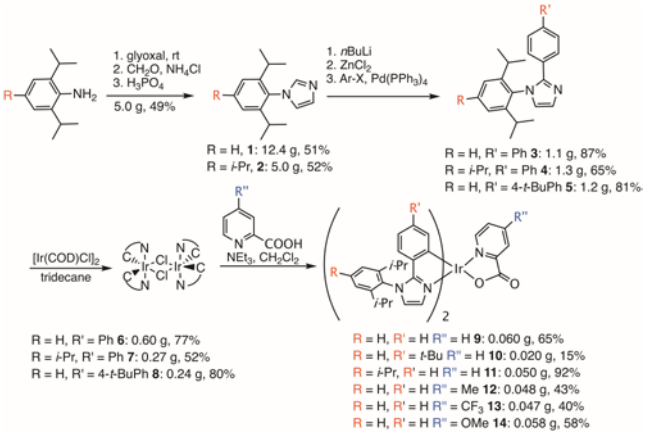

Scheme 1. Synthesis of Ir complexes **6**-**14**.

After synthesis and chromatography, X-Ray quality single crystals of complex **12** were grown from a concentrated solution of $CDCl_3$, and the solved structure is shown in Figure 2.

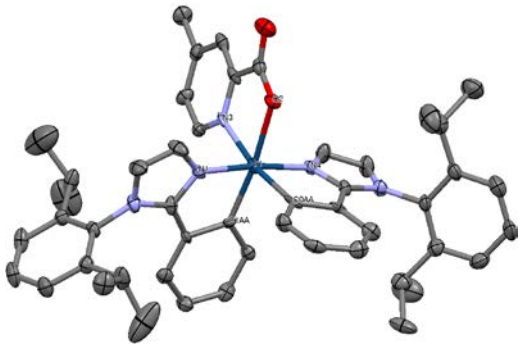

Figure 2. ORTEP Plot of the crystallographically determined structure of complex **12** (thermal probability ellipsoids drawn at the 50% confidence level). Hydrogen atoms are omitted for clarity. Selected bond distances: Ir1-O2: 2.155(5) Å, Ir1-N1: 2.010(8) Å, Ir1-N3: 2.117(7) Å, Ir1-N4: 2.018(8) Å, Ir1-C0AA: 1.978(8) Å, Ir1-C1AA: 1.973(7) Å. Selected Bond Angles: O2-Ir1-N1: 94.6(3)º, O2-Ir1-N3: 76.5(3)º, O2-Ir1-N4: 90.3(3)º, O2-Ir1-C0AA: 96.5(3)º, O2-Ir1-C1AA: 173.1(3)º, N3-Ir1-N4: 92.1(3)º, N1-Ir1-C1AA: 80.1(3)º, N4-Ir1-C0AA: 80.0(3)º, N1-Ir1-N4: 173.6(3)º, N3-Ir1-C0AA: 169.5(3)º, N3-Ir1-C1AA: 99.3(3)º

Details of SCXRD experiments are given in the Supporting Infomration, along with cif files. In the crystal structure of complex **12**, the Ir atom adopts the expected distorted octahedral geometry. Planar 2-arylimidazole ligands are perpendicular with chelating nitrogen atoms opposite to each other, which is also observed in $(ppy)_2Ir(pic)$ complexes.[22,23] Bond angles and distances were typical of other Ir (III) structures in a distorted octahedral, with no significant steric interactions.

Opto-Electronic Characterization

Once the complexes were synthesized, we characterized them by cyclic voltammetry to better understand the structure function relationship (Table 1, Figure 3). The complex with the least-accepting cyclometallating ligand, complex **10**, had the highest energy (destabilized) ground state oxidation potential ($E_{(S+/S)}$) value, while the complex with the least-accepting wingtip functionality, complex **11**, showed no change compared to the unmodified ligand of complex **9**, which indicated modification of the wingtip aryl group did not affect the molecular ground state. The complex with the most accepting picolinate ancillary ligand, complex **14**, displayed the lowest energy (most stabilized) $E_{(S+/S)}$. Decreasing the electron-accepting power of the picolinate complex through substitution with more inductive and resonance donating functional groups as in complexes **9**, **12**,**13** led to successively higher energy (destabilized) $E_{(S+/S)}$ values, which indicated that the picolinate directly affected the molecular ground state energy, as is the case for arylpyridine complexes like FIrPic.

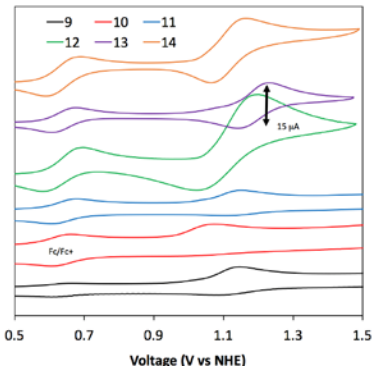

Figure 3. Measured in a 0.1 M Bu_4NPF_6 in MeCN solution with glassy carbon working electrode, Pt reference electrode, and Pt counter electrode with ferrocene as an internal standard. Values are reported versus NHE using the conversion Fc/Fc^+ = 0.64 V vs NHE in MeCN.[24]

Table 1. Electrochemical and Optical Properties of Ir Complexes 9-14.

Complex	E(S+/S) [a] (V vs NHE)	ε,[b] (10^4molL^{-1}cm^{-1})	λ_{max} [b] (nm)	E_{HOMO} [c] (eV Vs vacuum)	$E(T_1)$ [d] (eV Vs vacuum)
9	1.13	316 (1.32), 336 (1.30), 376 (0.75), 402 (0.53)	571	-5.73	-3.14
10	1.05	336 (1.54), 377, (0.98), 400 (sh, 0.74), 463 (0.025)	577	-5.65	-3.08

11	1.13	314 (1.11), 342 (0.94), 371 (sh, 0.57), 402 (0.33)	571	-5.73	-3.14
12	1.12	318 (1.64), 335 (sh, 1.49), 372 (0.90), 399 (0.61)	555	-5.72	-3.07
13	1.18	338 (1.28), 368 (1.13), 397 (sh,), 462 (0.12)	654	-5.78	-3.48
14	1.11	317 (1.50), 337 (sh, 1.27), 372 (0.79), 402 (0.54)	555	-5.71	-3.01

a: Measured in a 0.1 M Bu_4NPF_6 in MeCN solution with glassy carbon working electrode, Pt reference electrode, and Pt counter electrode with ferrocene as an internal standard. Values are reported versus NHE. b: Measured in degassed MeCN. c: Value obtained from the equation E_{HOMO} = -4.6 eV – $E_{(S+/S)}$ d: Value taken as the difference between E_{HOMO} and the high energy onset of the photoluminescence curve in degassed MeCN.

To understand how structural changes affected emission, we measured the UV-Vis and photoluminescence of each complex dissolved in MeCN (Table 1, Figure 4). Overall, the UV-Vis absorbance spectra looked qualitatively similar for each of the complexes, as was expected. Looking more closely at the spectra, subtle differences are apparent. For instance, compared to complex **9** (unmodified ligand) decreasing the electron accepting power of the cyclometallating ligand (complex **10)** increased absorptivity while modifying the imidazole wingtip (complex **11**) decreased absorptivity. Modifying the picolinate ligand with a methoxy functionality largely had no affect on the absorptivity, while trifuluoromethyl functionalization increased absorptivity and introduced a pronounced band at 460 nm.

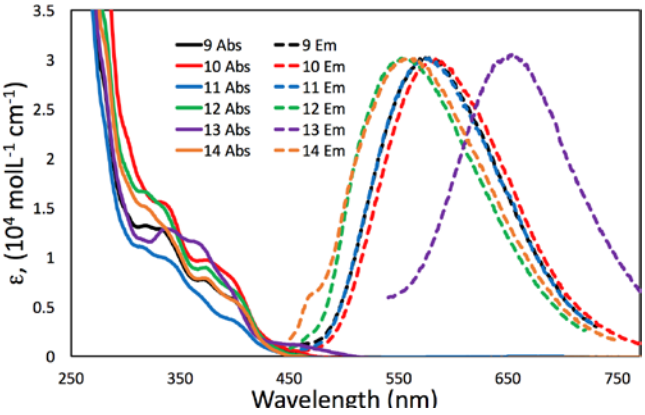

Figure 4. UV-Vis and Normalized Photoluminescence spectra of complexes **9**-**14** dissolved in Ar-saturated MeCN.

The steady-state photoluminescence spectra of complexes **9**-**14** in MeCN were measured to understand the changes to the emissive state upon ligand modification. Adding electron density to the cyclometallating ligand led to a slight red shift in the λ_{max} value (577 nm for **10** vs 571 nm for **9**) while modifying the imidazole wing-tip had no effect on λ_{max} (complex **11** vs **9**). Modifying the picolinate ligand was found to have a much more drastic effect, as increasing picoliate accepting power led to an 83 nm red shift (654 nm for complex **13** vs 571 nm for **9**). Decreasing accepting power through addition of methoxy or methyl led to a less-pronounced blue shift (17 nm) for both complexes (complexes **12**,**14** vs complex **9**). From the photoluminescence data, it is clear that picolinate ligand modifications affect emission more than absorption, and that the emission energy can be easily tuned by modifying the picolinate electron donation and acceptor strength. Because of its intrinsic accepting ability, the LUMO likely lies on the picolinate ligand, and this data supports this prediction, since emission energy should be lowered by increasing the accepting power of the LUMO-bearing moiety.[13]

Thus, from the electrochemical measurements it appeared that the molecular HOMO $E_{(S+/S)}$ was likely localized on the Ir and cyclometallating moiety of the imidazole ligand (as has been observed in calculations of homoleptic complexes)[14] and from the optical measurements it was apparent that the emissive triplet state $E_{(T1)}$was likely a mixed Ir-picolinate MLCT state, as is the case for FIrPic, with the difference of very little ligand-centered triplet state character in the emissive state, as evidenced by the featureless charge transfer band present for each complex.[8]

The energy levels of complexes **9**-**14** are compiled in Figure 5 for comparison. From the graph, the ramifications of ligand modification are easier to visualize, especially in the context of band-gap energy. For instance, adding electron density to the cyclometallating ligand in complex **10** destabilized the $E_{(S+/S)}$ energy level more than $E(T_1)$, lowering the band-gap energy. Conversely, in complex **12** and **13**, the $E_{(S+/S)}$ level was slightly destabilized, but $E(T_1)$ was destabilized to a greater degree, leading to overall band-gap widening. In complex **13**, both $E_{(S+/S)}$ and $E(T_1)$ were stabilized, with much more stabilization occurring at the $E(T_1)$ energy level.

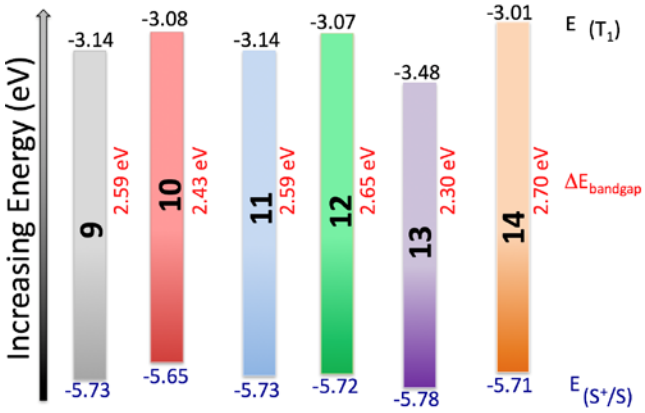

Figure 5. Energy Level Diagram for complexes **9**-**14**.

Once we had measured the relevant energy levels for each of the emitters, we then turned to gaining a better understanding of the time-dependent photophysical properties of the complexes. Our first set of measurements involved obtaining excited state lifetime and photoluminescence quantum yield (PLQY, Φ) data for the complexes (Table 2). The PLQY measurements were performed relative to FIrPic in DCE (PLQY = 92%), as described previously.[25,26] As has been described for a serious of recently published heteroleptic phenylpyridine acetylene-substituted picolinates, the observed PLQY values were much lower than those for FIrPic, but similar to those for $Ir(ppy)_2(pic)$ (14.7%).[23] Complex **12** exhibited the highest PLQY (24.7%) and complex **13** the lowest (6.4%). Complex **10** displayed higher PLQY than complexes **9** and **11**, and methoxy substituted complex **14**. Complexes **9**-**14** exhibited extremely weak oxygen-sensitive phosphorescence in MeCN, as has been described for other complexes, with excited state lifetimes near 10 ns.[27,28] With a similar trend to the quantum yields, the longest observed excited state was for complex **12** and the shortest for complex **13**. Even though the observed lifetimes are very low, similar lifetimes and quantum yields have been observed in cationic Ir complexes.[29] Thus, it was concluded that while substitution

on the cyclometallating moiety could boost PLQY (and thus the radiative rate constant), substitution on the wingtip aryl group had a detrimental effect. Similarly, while methyl substitution greatly enhanced PLQY, more electron rich methoxy and strongly accepting trifluoromethyl both decreased PLQY in comparison to complex **9**.

Table 2. Photophysical Properties of complexes **9**-**14**.[a]

Complex	**9**	**10**	**11**	**12**	**13**	**14**
PLQY (Φ, %)[b]	11.7	14.2	9.5	24.7	6.4	10.6
Excited State Lifetime (τ, μs)	0.012[c]	0.010[c]	0.011[c]	0.050	0.005	0.019

a: Values taken from measurements made in DCE. b: Measured relative to FIrPic.[25] c: Measurement made in degassed MeCN.

Conclusion

Finding new, more efficient emitters for OLEDs is an important challenge in chemistry, since lighting devices consume a large amount of energy worldwide. Towards this end, emitting molecules must be rationally designed to fit in to high performance device configurations. Towards the aim of a deeper understanding of the ramifications of emitter functionalization, we synthesized a series of heteroleptic bis(2-arylimidazole) iridum (III) picolinates with different steric and electronic modifications, from simple alkyl substitution on the cyclometallating ring or the imidazole wingtip group, to electronic modification of the picolinate ligand. The complexes were characterized by NMR and UV-Visible Absorption Spectroscopy, Photoluminescence Spectroscopy, Mass Spectrometry, and one complex was characterized by single crystal X-Ray Diffraction. It was determined that ligand substitution played a major role in the relative position of molecular energy levels (and thus emission wavelength), the observed photoluminescence quantum yield, and the excited state lifetime. Particularly, it was observed that functionalizing the picolinate ligand at the 4 position with a methyl group increased the PLQY and emission energy. Conversely, substitution at the 4 position with trifluoromethyl led to a large decrease in emission energy, and a decrease in PLQY. Studies such as these are important for establishing the structure-property relationship in various phosphorescent emitters for OLEDs, as better design rules will come from a larger pool of known complexes. Further studies into structure-property relationship in Ir (III) emitters are currently underway.

ASSOCIATED CONTENT

Supporting Information. The Supporting Information is available free of charge on the ACS Publications website. Selected Spectra and CIF files for crystal structures.

AUTHOR INFORMATION

Author Contributions

All authors have given approval to the final version of the manuscript.

Funding Sources

No competing financial interests have been declared.

ACKNOWLEDGMENT

The authors acknowledge SNSF NRP 70 project; number: 407040 154056, European Commission H2020-ICT-2014-1, SOLEDLIGHT project, grant agreement no.: 643791 and the Swiss State Secretariat for Education, Research and Innovation (SERI), and CTI 15864.2 PFNM-NM, the HZB-HU Graduate School "hybrid4energy," and Solaronix, Aubonne, Switzerland. A.H. acknowledges support from special funding for energy research, managed by Prof. Andreas ZÜTTEL, Funds no. 563074.

REFERENCES

(1) Baldo, M. A. A.; Lamansky, S.; Burrows, P. E. E.; Thompson, M. E. E.; Forrest, S. R. R. *Appl. Phys. Lett. 4*.

(2) Adachi, C.; Baldo, M. A.; Thompson, M. E.; Forrest, S. R.; Adachi, C.; Baldo, M. A.; Thompson, M. E.; Forrest, S. R. **2010**, *5048* (2001).

(3) Yersin, H.; Rausch, A. F.; Czerwieniec, R.; Hofbeck, T.; Fischer, T. *Coord. Chem. Rev.* **2011**, *255* (21–22), 2622.

(4) Baldo, M. a.; O'Brien, D. F.; Forrest, S. R.; O'Brien, D. F.; Thompson, M. E.; Forrest, S. R. *Phys. Rev. B* **1999**, *60* (20), 14422.

(5) Papi, K.; Zanoni, S.; Coppo, R. L.; Amaral, R. C. *Dalt. Trans.* **2015**, *44*, 14559.

(6) Thompson, M. *MRS Bull.* **2007**, *32* (September), 694.

(7) Baranoff, E.; Curchod, B. F. E.; Monti, F.; Steimer, F.; Accorsi, G.; Tavernelli, I.; Rothlisberger, U.; Scopelliti, R.; Grätzel, M.; Nazeeruddin, M. K. *Inorg. Chem.* **2012**, *51* (2), 799.

(8) Baranoff, E.; Curchod, B. F. E. *Dalt. Trans.* **2015**, *44* (18), 8318.

(9) Lee, J.; Chen, H.-F.; Batagoda, T.; Coburn, C.; Djurovich, P. I.; Thompson, M. E.; Forrest, S. R. *Nat. Mater.* **2016**, *15*, 92.

(10) Klubek, K. P.; Dong, S.-C. C.; Liao, L.-S. S.; Tang, C. W.; Rothberg, L. J. *Org. Electron. physics, Mater. Appl.* **2014**, *15* (11), 3127.

(11) Zhuang, J.; Li, W.; Wu, W.; Song, M.; Su, W.; Zhou, M.; Cui, Z. *New J. Chem.* **2015**, *39* (1), 246.

(12) Li, J.; Djurovich, P. I.; Alleyne, B. D.; Yousufuddin, M.; Ho, N. N.; Thomas, J. C.; Peters, J. C.; Bau, R.; Thompson, M. E. *Inorg. Chem.* **2005**, *44* (6), 1713.

(13) Huckaba, A. J.; Nazeeruddin, M. K. *Comments Inorg. Chem.* **2016**, *0* (ja), 1.

(14) Li, J.; Wang, L.; Sun, K.; Zhang, J. *Dalt. Trans.* **2016**, *45* (7), 3034.

(15) Zhuang, J.; Li, W.; Su, W.; Liu, Y.; Shen, Q.; Liao, L.; Zhou, M. *Org. Electron.* **2013**, *14* (10), 2596.

(16) Udagawa, K.; Sasabe, H.; Cai, C.; Kido, J. *Adv. Mater.* **2014**, *26* (29), 5062.

(17) Jayabharathi, J.; Thanikachalam, V.; Saravanan, K.; Perumal, M. V. *Spectrochim. Acta Part A Mol. Biomol. Spectrosc.* **2012**, *91*, 158.

(18) Jayabharathi, J.; Thanikachalam, V.; Srinivasan, N.; Perumal, M. V. *J. Fluoresc.* **2011**, *21* (4), 1585.

(19) Still, W. C.; Kahn, M.; Mitra, A. *J. Org. Chem.* **1978**, *43* (14), 2923.

(20) Liu, J.-Y.; Zheng, Y.; Li, Y.-G.; Pan, L.; Li, Y.-S.; Hu, N.-H. *J. Organomet. Chem.* **2005**, *690* (5), 1233.

(21) Micksch, M.; Tenne, M.; Strassner, T. *European J. Org. Chem.* **2013**, *2013* (27), 6137.

(22) Frey, J.; Curchod, B. F. E.; Scopelliti, R.; Tavernelli, I.; Rothlisberger, U.; Nazeeruddin, M. K.; Baranoff, E. *Dalton Trans.* **2014**, *43* (15), 5667.

(23) Davidson, R.; Hsu, Y.; Bhagani, C.; Yu, D.; Beeby, A. **2017**, ASAP.

(24) Connelly, N. G.; Geiger, W. E. *Chem. Rev.* **1996**, *96* (2), 877.

(25) Endo, A.; Suzuki, K.; Yoshihara, T.; Tobita, S.; Yahiro, M.; Adachi, C. *Chem. Phys. Lett.* **2008**, *460* (1–3), 155.

(26) Aghazada, S. S.; Huckaba, A. J.; Pertegas, A.; Babaei, A.; Grancini, G.; Zimmermann, I.; Bolink, H.; Nazeeruddin, M. K. *Eur. J. Inorg. Chem.* **2016**, *2016* (32), 5089.

(27) Takizawa, S.; Ikuta, N.; Zeng, F.; Komaru, S.; Sebata, S.; Murata, S. *Inorg. Chem.* **2016**, *55* (17), 8723.

(28) Ma, L.; Guo, H.; Li, Q.; Guo, S.; Zhao, J. *Dalt. Trans.* **2012**, *41* (35), 10680.

(29) Hasan, K.; Bansal, A. K.; Samuel, I. D. W.; Roldán-Carmona, C.; Bolink, H. J.; Zysman-Colman, E. **2015**, *5*, 12325.